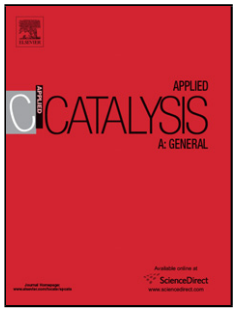

Title: Hydrogenolysis of glycerol over supported bimetallic Ni/Cu catalysts with and without external hydrogen addition in a fixed-bed flow reactor

Authors: Fufeng Cai, Donghui Pan, Jessica Juweriah Ibrahim, Jun Zhang, Guomin Xiao

PII: S0926-860X(18)30368-5
DOI: https://doi.org/10.1016/j.apcata.2018.07.029
Reference: APCATA 16755

To appear in: *Applied Catalysis A: General*

Received date: 8-4-2018
Revised date: 1-6-2018
Accepted date: 23-7-2018

Please cite this article as: Cai F, Pan D, Ibrahim JJ, Zhang J, Xiao G, Hydrogenolysis of glycerol over supported bimetallic Ni/Cu catalysts with and without external hydrogen addition in a fixed-bed flow reactor, *Applied Catalysis A, General* (2018), https://doi.org/10.1016/j.apcata.2018.07.029

Hydrogenolysis of glycerol over supported bimetallic Ni/Cu catalysts with and without external hydrogen addition in a fixed-bed flow reactor

Fufeng Cai,[a,b,] Donghui Pan,[b] Jessica Juweriah Ibrahim,[c] Jun Zhang,[a,*] Guomin Xiao[b]*

[a] *CAS Key Laboratory of Low-Carbon Conversion Science and Engineering, Shanghai Advanced Research Institute, Chinese Academy of Sciences, Shanghai 201210, China*

[b] *School of Chemistry and Chemical Engineering, Southeast University, Nanjing 211189, China*

[c] *Key Laboratory of Bio-based Material, Qingdao Institute of Bioenergy and Bioprocess Technology, Chinese Academy of Sciences, Qingdao 266101, China*

**Corresponding authors.*

E-mail: caiff@sari.ac.cn (F. Cai), zhangj@sari.ac.cn (J. Zhang). Tel./Fax: +86 21 20350994.

Graphical Abstracts

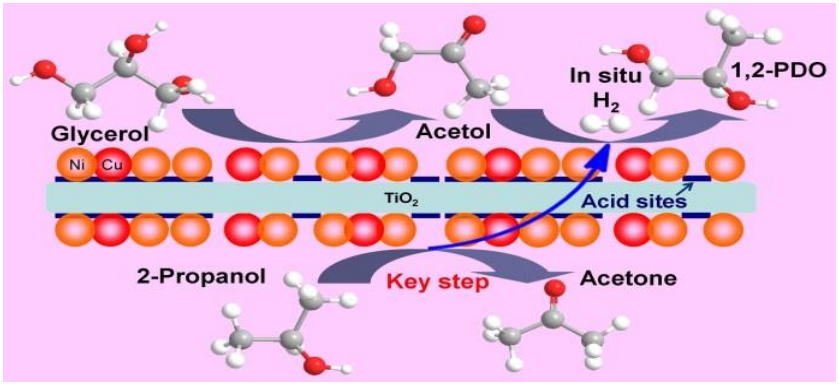

Highlights

- ● Ni/Cu/TiO_2 is effective for glycerol hydrogenolysis without external hydrogen supply
- ● Ni/Cu/TiO_2 showed the high Cu dispersion and Ni/Cu atomic ratio on catalyst surface
- ● Metal active sites of catalyst play a significant role on glycerol hydrogenolysis
- ● Ni/Cu/TiO_2 catalyst undergoes serious deactivation after certain time of running
- ● Deactivation is related to metal leaching, sintering and presence of adsorbed species

Abstract

The role of high hydrogen pressure in the hydrogenolysis of glycerol to 1,2-propanediol has been

studied extensively. Given the peculiar properties of hydrogen such as its inflammability and explosibility, the hydrogenolysis of glycerol without external hydrogen addition seems a more advantageous option. This study focuses on the conversion of glycerol to 1,2-propanediol over different supported bimetallic Ni/Cu catalysts in a fixed-bed flow reactor, using *in situ* hydrogen production and external hydrogen. Among the catalysts prepared, Ni/Cu/TiO_2 catalyst was observed to efficiently catalyze the hydrogenolysis of glycerol to 1,2-propanediol under N_2 pressure using 2-propanol as hydrogen source. This was due to the high Cu dispersion and Ni/Cu atomic ratio on the catalyst surface. However, the experimental results indicated that the effect of catalyst acid sites on glycerol hydrogenolysis was more noticeable when the reaction was performed under H_2 pressure. The metal active sites of the catalyst played a significant role in the hydrogen production and also affected the glycerol hydrogenolysis with hydrogen produced from 2-propanol catalytic transfer hydrogenation (CTH) and glycerol aqueous phase reforming (APR). The stability study revealed that the Ni/Cu/TiO_2 catalyst underwent serious deactivation during the hydrogenolysis of glycerol. The characterization results showed that the metal leaching and metal particles sintering were responsible for the catalyst deactivation when the glycerol hydrogenolysis was conducted using water as a solvent. However, the activity loss for reactions performed using 2-propanol as a solvent was mainly related to the metal particles sintering and the presence of adsorbed species on the catalyst surface.

Keywords: Glycerol; Hydrogenolysis; 1,2-Propanediol; 2-Propanol; Ni/Cu/TiO_2 catalyst

1. Introduction

With the increasing environmental concerns and diminishing traditional fossil fuels, biodiesel has attracted considerable attention in the past decade as an environmentally friendly and renewable biomass fuel [1]. Glycerol, a byproduct in the production of biodiesel, is available in surplus [2]. In this regard, many studies have focused on the transformation of glycerol into higher-value commodity chemicals by various catalytic conversion processes. Some of these processes include selective oxidation, esterification, etherification, carboxylation, hydrogenolysis, and so forth [3–6]. Particularly, the hydrogenolysis of glycerol to 1,2-propanediol (1,2-PDO) in the presence of metallic catalysts and hydrogen is one of the most promising methods for effective utilization of glycerol [7].

Generally, high H_2 pressure is necessary to obtain a satisfactory catalytic performance during the glycerol hydrogenolysis process [8]. There are, however, potential hazards for the use of molecular hydrogen because of its peculiar properties, *e.g.*, high diffusivity, inflammability and explosibility, especially when working at high pressure. Furthermore, most of the available hydrogen gas currently is mainly generated from fossil feedstock. Fortunately, *in situ* hydrogen production and simultaneous consumption in the hydrogenolysis of glycerol can overcome the inherent disadvantages of the use of molecular hydrogen [9]. In accordance with this idea, two different catalytic processes have been explored in the hydrogenolysis of glycerol without providing molecular hydrogen from an external source, *i.e.*, catalytic transfer hydrogenation (CTH) and aqueous phase reforming (APR) (see Scheme 1) [10,11].

So far, the glycerol hydrogenolysis with hydrogen produced from CTH, where hydrogen is shifted from the hydrogen donors to the acceptors, has been deeply explored by several research

groups. Musolino et al. [12] tested the catalytic performance for glycerol hydrogenolysis with hydrogen produced from the dehydrogenation of ethanol and 2-propanol over a Pd/Fe_2O_3 catalyst. They found that the best catalytic result was obtained in the presence of 2-propanol as hydrogen donor. Xia et al. [13] studied the conversion of glycerol to 1,2-PDO over Cu-Mg-Al catalysts with hydrogen generated from the different alcohols. They noted that ethanol was the best hydrogen donor molecular. In 2012, Gandarias and co-workers [14,15] systematically investigated the activity for glycerol hydrogenolysis and CTH reaction on $Ni-Cu/Al_2O_3$ catalyst using formic acid as a solvent. The authors claimed that both acid and metal sites on the catalyst played key roles in glycerol hydrogenolysis with hydrogen produced from formic acid CTH, because the glycerol molecules were easily adsorbed on the acid sites of support while the activation of hydrogen occurred on the surface of metal sites.

In the case of APR, the hydrogen is first produced from the reforming process and subsequently reacts with glycerol to form 1,2-PDO. In 2008, D'Hondt et al. [16] first studied the catalytic activity for 1,2-PDO production from glycerol conversion on different supported Pt catalysts with hydrogen derived from glycerol APR. They declared that the best catalytic activity was achieved in the existence of Pt/NaY catalyst, and attributed this result to a good balance between the metal and acid sites in Pt/NaY catalyst. After the study of D'Hondt et al., some other researchers have also examined the catalytic activity of coupling glycerol APR with hydrogenolysis. Mauriello et al. [17] tested the activity for glycerol APR and hydrogenolysis over the bimetallic Pd/Fe catalyst. It achieved 100% of glycerol conversion and 43% of 1,2-PDO selectivity at 210 ℃, 5 bar He and 24 h reaction time. Pendem et al. [18] found that the use of hydrotalcite as a support was beneficial to the formation of highly dispersed Pt particles, and Pt/hydrotalcite catalyst exhibited 69% 1,2-PDO

yield when using water as the reaction medium at 250 ℃ and 4.5 MPa of N_2 pressure.

Except for the noble metal catalysts, different non-noble metal, such as Ni and Cu, catalysts were also used in glycerol hydrogenolysis with hydrogen generated from APR. Seretis et al. [19] investigated the activity of glycerol hydrogenolysis with hydrogen produced from glycerol APR over $Ni/SiO_2/Al_2O_3$ catalyst. It resulted in a 22% 1,2-PDO yield at 240 ℃ and 4 h batch test. Yun et al. [20] found that incorporation of Ni into mesoporous alumina supported Cu catalyst can significantly increase the activity of glycerol hydrogenolysis and hydrogen production via APR of glycerol. Similarly, Freitas et al. [21] in their study claimed that bimetallic $CuNi/Al_2O_3$ and CuNi/ZSM-5 catalysts showed superior activity of glycerol hydrogenolysis with hydrogen produced from glycerol APR. They attributed this result to the presence of Cu-Ni alloy interaction, high acidity and good metal dispersion on the catalyst surface.

Despite much research work has been done as stated above, there still exist some disadvantages such as the use of noble metal catalysts and poor catalytic activity in non-noble metal catalyst for glycerol hydrogenolysis with hydrogen generated from APR or CTH. Furthermore, it should be noted that most of the research on glycerol hydrogenolysis without external hydrogen addition were performed at a batch reactor, in which high pressure and long reaction time were necessary [19,20]. According to literature, Ni catalysts provide a good activity in hydrogen production, while Cu catalysts show a high activity in the C–O bond hydrogenolysis [15]. Therefore, the bimetallic Ni/Cu catalyst seems especially suitable for the conversion of glycerol to 1,2-PDO when there is *in situ* hydrogen production. In the present work, different supported bimetallic Ni/Cu catalysts were prepared and used for 1,2-PDO production from glycerol in a fixed-bed flow reactor, aided by *in situ* hydrogen production and also with external hydrogen supply. The roles of acid and

metal sites of the catalysts on the catalytic activity for glycerol conversion to 1,2-PDO were intensively investigated. In addition, the influences of different reaction parameters on glycerol hydrogenolysis and catalyst stability characteristics were also explored.

2. Experimental

2.1. Catalyst preparation

The supported bimetallic Ni/Cu catalysts were prepared by incipient wetness impregnation of the supports, *i.e.*, γ-Al_2O_3 (100-200 mesh, S_{BET} = 231 $m^2 \cdot g^{-1}$, Nanjing Chemical Reagent CO., Ltd., China), CeO_2 (Sinopharm Chemical Reagent Co., Ltd., China (SCRC)), SiO_2 (Qingdao Ocean Chemical CO., Ltd., China), TiO_2 (SCRC), ZrO_2 (SCRC), or HZSM-5 (Si:Al = 40) (Nankai University Catalyst CO., Ltd., China), with aqueous solutions that contained a certain amount of nickel nitrate and copper nitrate. Following the general procedure, 7.43 g of nickel nitrate hexahydrate and 3.80 g of copper nitrate hydrate were dissolved in a certain amount of deionized water and dispersed for 60 min at 40 ℃ with an ultrasonic machine (40KHz, 100W). Subsequently, the mixed solution was vigorously stirred (900 rpm) by a mechanical stirrer at 40 ℃ for 180 min, and then 5.0 g of support was added to the mixed solution and continuously stirred at 40 ℃ for two days. After impregnation, the water was eliminated by heating and stirring at 95 ℃ under vacuum by means of a rotary evaporator. Then, the solid mixture was dried at 110 ℃ for overnight in an oven and calcined at 400 ℃ for 240 min in a muffle furnace with a stationary air atmosphere. The bimetallic Ni/Cu catalysts obtained were ground with an agate mortar and pressed by a tablet machine at 10 MPa to form particles with sizes of 20 to 40 meshes. Unless otherwise stated, the nominal mass loadings for Ni and Cu on the support were fixed at 30 wt%

and 20 wt%, respectively. In addition, the monometallic catalysts, Ni/TiO_2 and $30Cu/TiO_2$, were also prepared by following the aforementioned procedure in order to ensure a comparative analysis.

2.2. Catalyst characterization

The actual contents of Ni and Cu in the prepared catalysts were determined with inductively coupled plasma optical emission spectroscopy (Optima 7300 DV, PerkinElmer). The specific surface area and pore volume of the supported bimetallic Ni/Cu catalysts were examined through nitrogen adsorption-desorption at -196 ℃ using a Beishide 3H-2000PS1 instrument. The morphological analysis of the supported bimetallic Ni/Cu catalysts was carried out with a scanning electron microscope (Philips XL-30 ESEM) operating at 15 kV. The transmission electron microscope image of the catalyst was achieved by using a transmission electron microscope (FEI Tecnai G2) with an operating voltage of 200 kV. The phase composition and surface chemical elements of the supported bimetallic Ni/Cu catalysts were analyzed respectively with an X-ray diffractometer (Bruker D8-Discover) with a Cu Kα radiation source at 40 kV and 30 mA, and an X-ray photoelectron spectrometer (ESCALAB 250Xi) with a Mg Kα radiation source. N_2O chemisorption was done to assess the Cu dispersion on the supported bimetallic Ni/Cu catalysts. The reducibility and acidity of the supported bimetallic Ni/Cu catalysts were determined by means of H_2-TPR and NH_3-TPD, respectively. The weight loss of the spent catalyst was measured by thermogravimetric analysis (SDT-Q600). The detailed procedures for the above-mentioned characterization methods have been shown in our previous work [22–24].

2.3. Catalytic activity test

The hydrogenolysis of glycerol was performed using a vertical fixed-bed flow reactor with an inside diameter of 1.1 cm and a length of 95 cm under specified conditions of temperature and pressure (see Figure S1). In a specific test, 6.0 g of the supported bimetallic Ni/Cu catalyst with particles sizes from 20 to 40 meshes was put into the central region (corresponding to constant temperature zone of reactor) of the stainless steel reaction tube, filled with quartz sand with particles sizes from 20 to 40 meshes at both ends. Prior to the catalytic activity test, the supported bimetallic Ni/Cu catalyst was *in situ* reduced in the fixed-bed flow reactor at 400 ℃ and 0.5 MPa of hydrogen pressure for 120 min with a flowing hydrogen (100 $mL \cdot min^{-1}$). After reduction, the temperature of reactor controlled with a computer temperature controller was decreased from 400 to 230 ℃ under the flowing hydrogen. Subsequently, the reactor was purged with a flowing nitrogen (50 $mL \cdot min^{-1}$) for 0.5 h to remove the hydrogen inside the reactor, and the whole reaction system was pressurized to 3.5 MPa of nitrogen pressure with a back pressure regulator. Next, a mixture of 5 wt% glycerol in 2-propanol (or water) preheated to 230 ℃ by a preheater was transported into the reactor with a feed rate of 27.8 $mL \cdot h^{-1}$ by using a metering pump along with co-feeding flowing N_2 (50 $mL \cdot min^{-1}$). In addition, the influences of reaction temperature, glycerol concentration and feed rate of liquid mixture were investigated respectively by varying the process parameters in the ranges of 180–250 ℃, 5–40 wt% and 13.2–58.7 $mL \cdot h^{-1}$.

After a certain time of running (*ca.* 60 min), the reaction products at reactor outlet were condensed (T = 0 ℃) and subsequently collected in a gas–liquid separator. The gas products that flowed out of the top of separator were analyzed off-line by means of a gas chromatograph (Tenghai GC-6890, China), equipped with a TCD and two chromatographic columns (OV-101 and 13X-5A). For the analysis of gas products, sample 2-3 times for each test point every 20 minutes

at the same reaction conditions, the sampling quantity is 0.5 L. The liquid products were taken from the bottom of separator and measured by means of a temperature programming gas chromatography (Shimadzu GC-2014) using 1,4-butanediol as an internal standard substance. This gas chromatography was equipped with a FID, and the capillary column was Rtx-WAX (30 m × 0.25 mm). In the case of liquid products analysis, sample 3-4 times for each experimental data every 20 minutes at the same reaction conditions, the sampling quantity is 10 mL. Each gas and liquid samples were analyzed two times by gas chromatography. The experimental results were the average values of data collected. In addition, the liquid products collected in the separator were determined by GC-MS (Shimadzu GCMS-QP2010) and submitted to ICP-OES analysis. The glycerol conversion and product selectivity were defined in equations (1) and (2), respectively. In this work, the values of carbon balance for glycerol hydrogenolysis were higher than 95% for each data acquisition and analysis. The uncertainties of the measurements for glycerol conversion and product selectivity were 1% and 2%, respectively.

$$\text{Conversion}\ (\%) = \frac{\text{moles of glycerol (in)} - \text{moles of glycerol (out)}}{\text{moles of glycerol (in)}} \times 100 \quad (1)$$

$$\text{Selectivity}\ (\%) = \frac{\text{moles of carbon in a specific product}}{\text{moles of carbon in glycerol consumed}} \times 100 \quad (2)$$

3. Results and discussion

3.1. Catalyst characterization

The physicochemical properties of supported bimetallic Ni/Cu catalysts measured using different characterization methods are listed in Table 1. As can be seen, Ni/Cu/γ-Al_2O_3, Ni/Cu/SiO_2 and Ni/Cu/HZSM-5 catalysts showed high BET surface area and pore volume,

whereas those of CeO_2, TiO_2 and ZrO_2 supported bimetallic Ni/Cu catalysts were considerably lower. This might be due to the nature of supports. However, the differences of the actual contents of Ni and Cu in the supported catalysts determined by ICP-OES were quite modest, and they were close to the theoretical ones. In order to identify the Cu dispersion of supported bimetallic Ni/Cu catalysts, N_2O chemisorption was carried out. As shown in Table 1, the Cu dispersion of $Ni/Cu/SiO_2$ catalyst was the lowest compared with the other supported bimetallic Ni/Cu catalysts. Instead, the $Ni/Cu/TiO_2$ catalyst possessed the highest Cu dispersion (10.4%) and lowest Cu particle size (9.6 nm), which might be related to the property of TiO_2, consistent with literature reports [25,26].

Table 1 Physicochemical properties of supported bimetallic Ni/Cu catalysts

Catalyst	S_{BET}[a] ($m^2 \cdot g^{-1}$)	V_p[a] ($cm^3 \cdot g^{-1}$)	Ni content[b] (wt%)	Cu content[b] (wt%)	D_{Cu}[c] (%)	S_{Cu}[c] ($m^2 \cdot g^{-1}$)	d_{Cu}[c] (nm)	Ni/Cu[d]	Acidity[e] (μmol $NH_3 \cdot g^{-1}$) 150-750 ℃	Acidity[e] (μmol $NH_3 \cdot g^{-1}$) 420-750 ℃
$Ni/Cu/\gamma\text{-}Al_2O_3$	206	0.564	27.2	17.0	5.1	34.5	19.6	1.13	684	454
$Ni/Cu/CeO_2$	35	0.121	26.9	16.8	7.0	47.4	14.3	0.97	105	89
$Ni/Cu/SiO_2$	236	0.833	27.8	16.7	3.4	23.0	29.4	0.90	97	37
$Ni/Cu/TiO_2$	54	0.135	27.5	17.0	10.4	70.4	9.6	1.30	197	156
$Ni/Cu/ZrO_2$	28	0.094	26.4	17.1	9.3	62.9	10.8	1.03	102	85
Ni/Cu/HZSM-5	229	0.197	27.7	17.9	8.6	58.2	11.6	1.27	630	366

[a] Tested from BET. [b] Tested from ICP-OES. [c] Tested from N_2O chemisorption. [d] Atomic ratio Ni/Cu obtained from XPS. [e] Tested from NH_3-TPD.

Figure 1 displays the SEM images of supported bimetallic Ni/Cu catalysts. It was evident that, with the exception of $Ni/Cu/SiO_2$, all the supported bimetallic Ni/Cu catalysts had blocky texture

with many particles deposited on the surface. Particularly, more small granules were present on the Ni/Cu/TiO_2 catalyst, showing its superior structure. In contrast, the microstructure of Ni/Cu/SiO_2 catalyst was spherical in shape with large numbers of floccose granules attached to the surface.

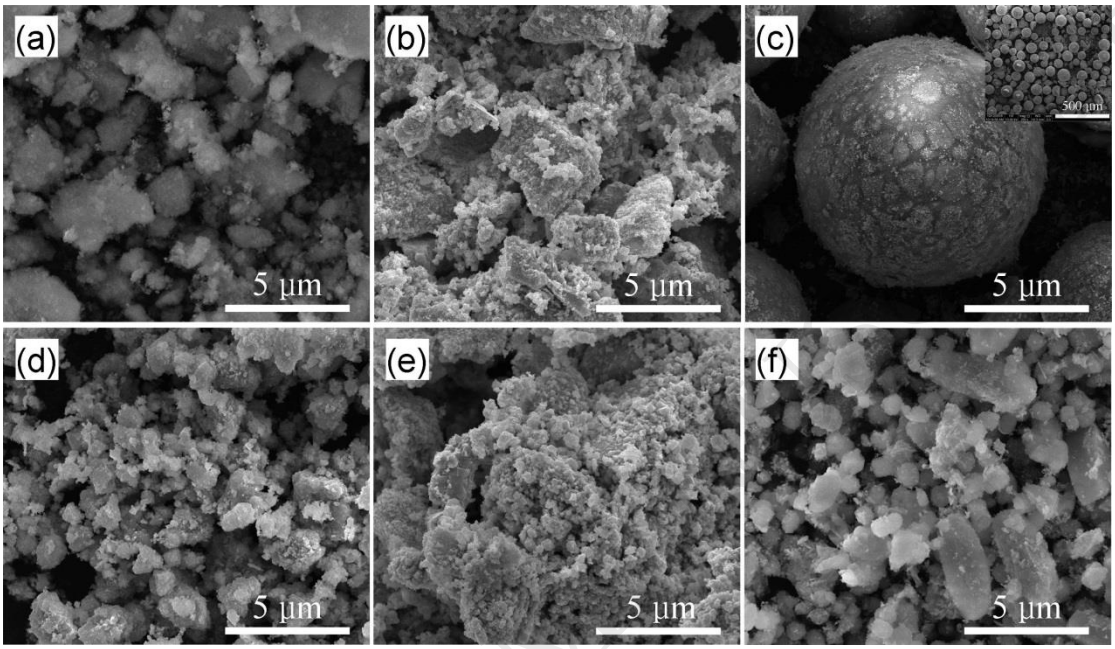

Figure 1. SEM images of supported bimetallic Ni/Cu catalysts: Ni/Cu/γ-Al_2O_3 (a), Ni/Cu/CeO_2 (b), Ni/Cu/SiO_2 (c), Ni/Cu/TiO_2 (d), Ni/Cu/ZrO_2 (e), and Ni/Cu/HZSM-5 (f).

The XRD patterns of supported bimetallic Ni/Cu catalysts upon calcination and reduction are illustrated in Figure 2. It is clear that, the presence of NiO (PDF#44-1159) gave rise to diffraction peaks for the calcined supported bimetallic Ni/Cu catalysts at 2θ = 37.2°, 43.3° and 62.8°, and the diffraction peaks at about 35.5°, 38.7° and 48.9° were assigned to CuO phase (PDF#48-1548) [21,27]. The diffraction peaks of both NiO and CuO phases were detected in all calcined supported Ni/Cu catalysts except for that of corresponding supports. After reduction, the diffraction peaks of NiO and CuO phases were not observed in all supported bimetallic Ni/Cu catalysts. Instead, the sharp diffraction peaks that can be ascribed to Cu (PDF#04-0836, 2θ = 43.3°,

50.4° and 74.1°) and Ni (PDF#01-1258, 2θ =44.4° and 51.6°) were detected, indicating that the NiO and CuO species existing in the calcined Ni/Cu catalysts were reduced to active metals Ni and Cu, respectively [21,27].

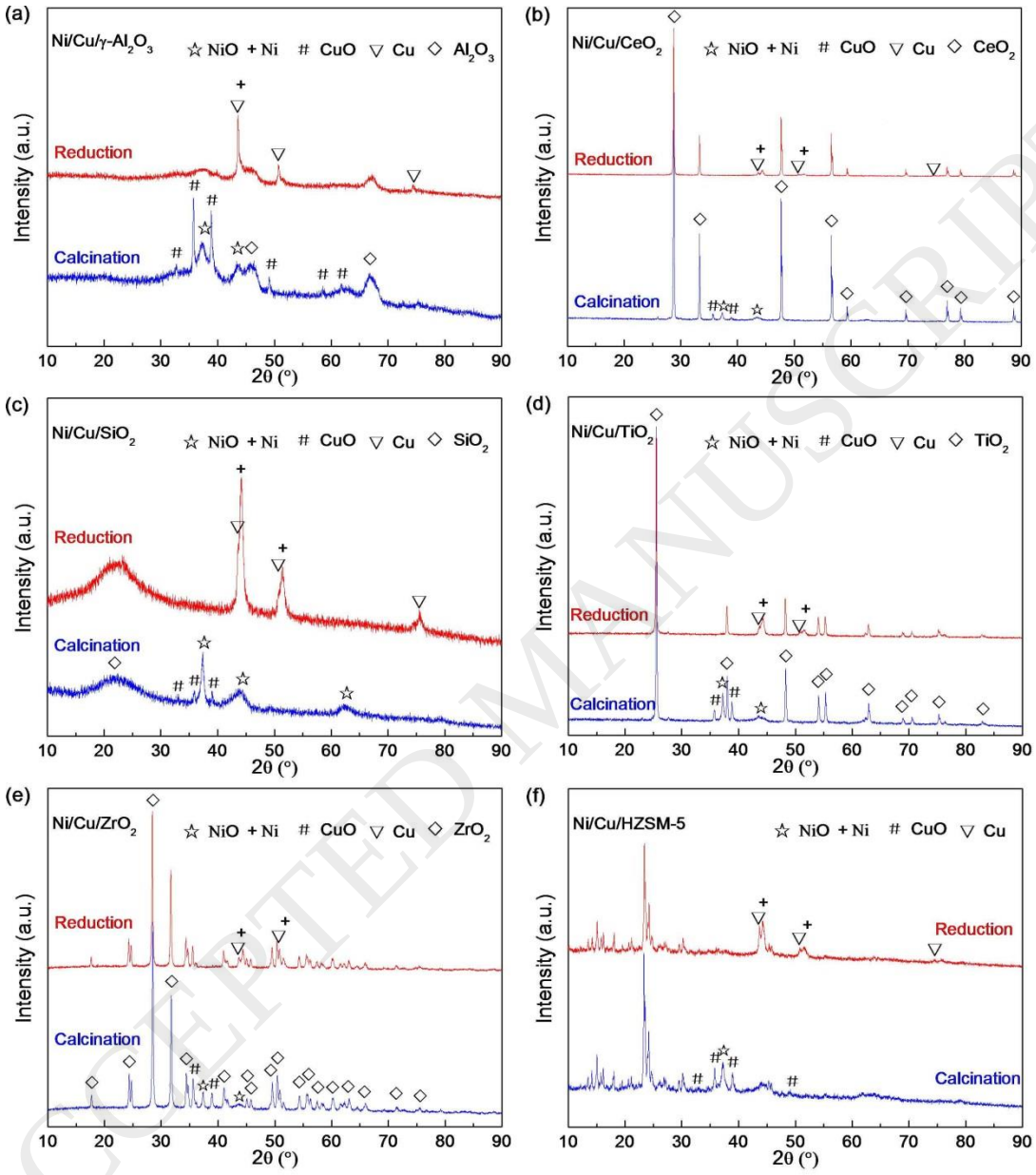

Figure 2. XRD patterns of supported bimetallic Ni/Cu catalysts.

Figure 3 shows the H_2-TPR profiles of supported bimetallic Ni/Cu catalysts. In Figure 3, the Ni/Cu/γ-Al_2O_3 catalyst exhibited two hydrogen consumption peaks, one at about 226 ℃ and the other at about 352 ℃. According to the study of Cu catalysts [28], the hydrogen consumption

peak in a lower temperature was considered to be the reduction of small CuO clusters distributed on the catalytic surface, while the high temperature peak indicated the reduction of bulk CuO particles. Based on this explanation, the hydrogen consumption peak of Ni/Cu/γ-Al_2O_3 catalyst at about 352 ℃ might be attributed to the reduction of bulk CuO with a larger size. However, it should be pointed out that the presence of Cu was beneficial to the reduction of NiO species and there was a spillover effect on Cu-Ni bimetallic catalysts [20,21]. As a result, the reduction temperature of NiO species can be greatly decreased. For this reason, it cannot be ruled out that the high temperature peak at about 352 ℃ may also describe the reduction of NiO species, which can be reduced below at 420 ℃ [21]. It was clear from Figure 3 that the reduction profiles of the other supported bimetallic Ni/Cu catalysts were different from that of Ni/Cu/γ-Al_2O_3 catalyst. Only one strong hydrogen consumption peak in the temperature range from 200 to 350℃ was noted. This behavior that there was only one reduction peak in the bimetallic Ni/Cu catalysts has also been reported in the literature [20,21]. It was evident that the reduction peak in the range of 200 to 350 ℃ was attributed to the reduction of CuO species. However, this hydrogen consumption peak might also include the reduction of NiO species. To illustrate this, TPD experiments for monometallic 30Cu/TiO_2 and Ni/TiO_2 catalysts were carried out. In Figure 3, the 30Cu/TiO_2 catalyst exhibited a strong hydrogen consumption peak at 150-300 ℃, which was related to the reduction of Cu^{2+} to Cu^0. Similarly, only a small peak centered at about 600 ℃ corresponding to the reduction of NiO species was observed on the Ni/TiO_2 catalyst. This again showed that the existence of Cu species for Ni/Cu/TiO_2 catalysts favored the reduction of NiO species, leading to a decrease in its reduction temperature.

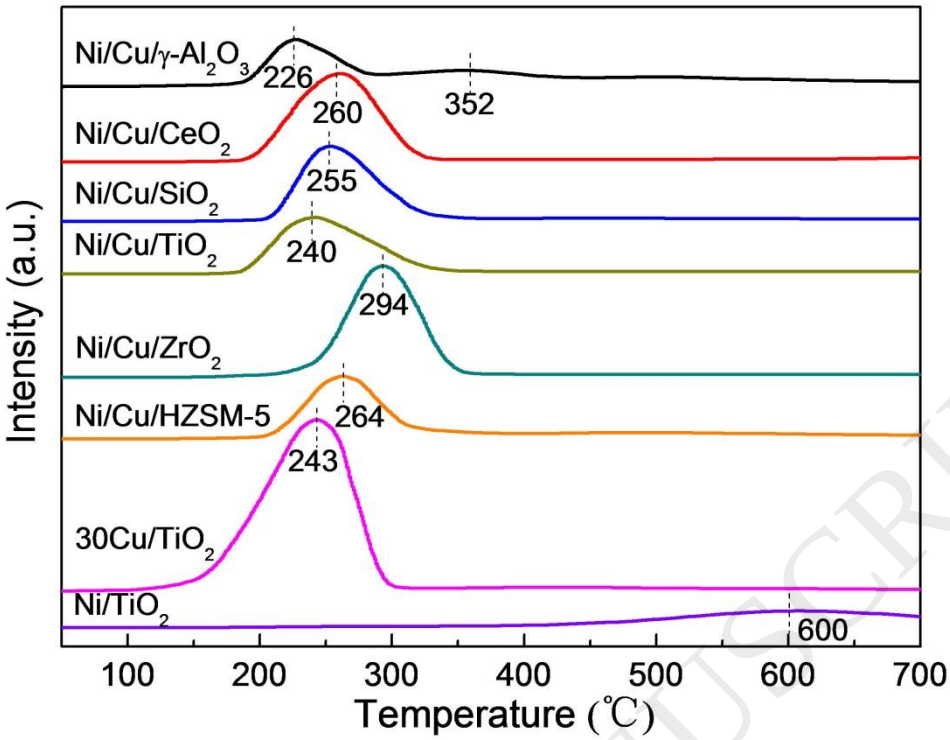

Figure 3. H_2-TPR profiles of supported bimetallic Ni/Cu catalysts.

The acidities of bare supports and supported bimetallic Ni/Cu catalysts were characterized by NH_3-TPD, and the results are shown in Figure S2 and Figure 4, respectively. The test results showed that the acidity of Ni/Cu/HZSM-5 catalyst was lower than that of bare support HZSM-5, consistent with report in the literature [21]. In contrast, there was a small increase of the acidity for other supported bimetallic Ni/Cu catalysts when compared to the corresponding bare supports, which might be due to the fact that the incorporation of metal species enhanced the amount of acid sites of catalysts [29,30]. According to previous reports [31,32], the acid sites of catalyst include weak acid, medium acid, and strong acid strength that correspond to the NH_3 desorption peak in the temperature range of 150–250, 250–420, and 420–750 ℃, respectively. It can be observed from Figure 4 that both Ni/Cu/γ-Al_2O_3 and Ni/Cu/HZSM-5 catalysts exhibited two intense NH_3 desorption peaks at 150–400 and 450–750 ℃ respectively, suggesting the presence of high concentration of acid sites. Additionally, the Ni/Cu/SiO_2 catalyst only showed a weak NH_3

desorption peak at 150–300 ℃, indicating that there existed a few weak acid sites. Unlike the $Ni/Cu/SiO_2$ catalyst, a small NH_3 desorption peak at high temperature (450–750 ℃) was seen on $Ni/Cu/CeO_2$, $Ni/Cu/TiO_2$ and $Ni/Cu/ZrO_2$ catalysts, showing the existence of some strong acid sites on these catalysts. For comparison, Table 1 shows the acidities of supported bimetallic Ni/Cu catalysts. It is clear from the data in Table 1 that the $Ni/Cu/\gamma\text{-}Al_2O_3$ catalyst possessed the highest concentration of acid sites, whereas the acid strength of $Ni/Cu/SiO_2$ catalyst was the lowest.

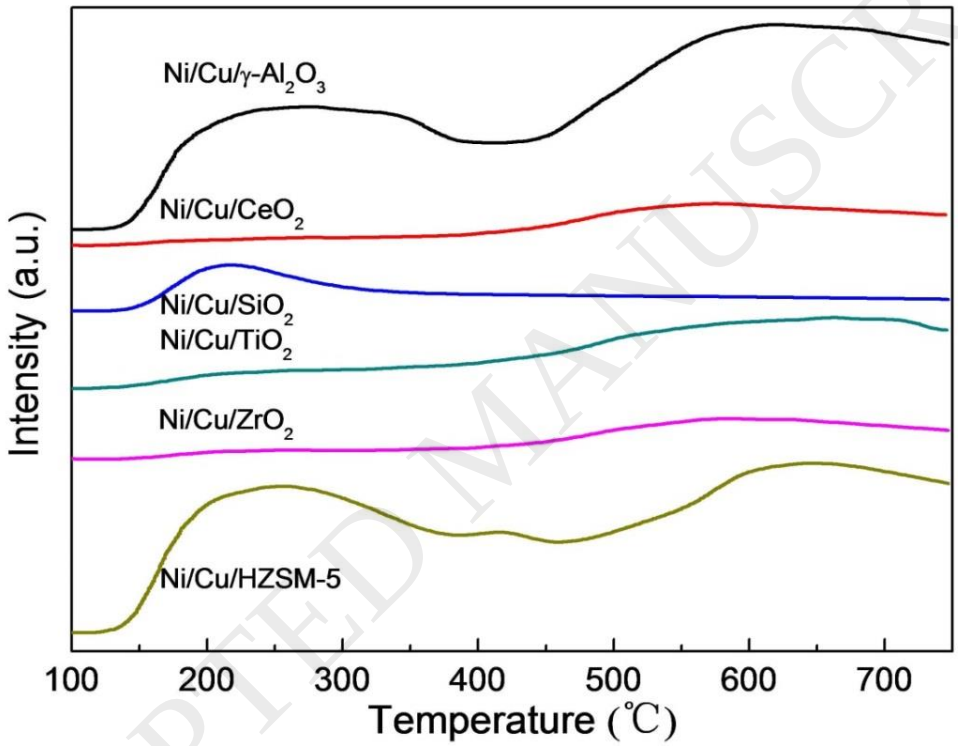

Figure 4. NH_3-TPD profiles of supported bimetallic Ni/Cu catalysts.

As illustrated in Figure 5, XPS analysis was carried out to gain further insight into the nature and surface composition information of metal species on the reduced catalysts. In Figure 5a, two strong peaks centered at about 932.2 and 952.2 eV respectively associated with Cu $2p_{3/2}$ and Cu $2p_{1/2}$ peaks of Cu^0 were evident in all supported bimetallic Ni/Cu catalysts [33]. Also, the absence of satellite peaks at about 943 and 963 eV corresponding to the spectra of Cu^{2+} species in CuO were noted, demonstrating that the Cu^{2+} species in the bimetallic Ni/Cu catalysts were fully

reduced to Cu^0 [28]. This conforms to the result of XRD analysis. In Figure 5b, the Ni 2p spectra of reduced bimetallic Ni/Cu catalysts can be separated into two categories: two weak peaks centered at *ca.* 852.4 and 869.6 eV respectively ascribed to Ni $2p_{3/2}$ and Ni $2p_{1/2}$ of Ni^0, and two strong peaks centered at *ca.* 855.8 and 873.5 eV respectively attributed to Ni $2p_{3/2}$ and Ni $2p_{1/2}$ of Ni^{2+} species in NiO [34]. Meanwhile, two strong satellite peaks were observed at *ca.* 862 and 880 eV, suggesting that only a certain percentage of Ni^{2+} species was reduced to Ni^0, and the Ni^{2+} and Ni^0 species coexisted in the reduced bimetallic Ni/Cu catalysts [20]. It is worthy to mention, however, that no obvious characteristic peaks corresponding to NiO species were detected on XRD analysis for the reduced bimetallic Ni/Cu catalysts, which might be attributed to the residual Ni^{2+} species highly dispersed on the catalyst surface. This behavior has been published elsewhere for other similar CuNi catalysts [20,21]. The surface Ni/Cu atomic ratios obtained from XPS analysis are summarized in Table 1. It should be noted that all surface Ni/Cu atomic ratios of bimetallic Ni/Cu catalysts were lower than the corresponding actual ones (1.6–1.8), which may be due to the fact that parts of well dispersed Ni species were covered by bulk Cu particles. Nonetheless, it was found that the Ni/Cu/TiO_2 catalyst possessed the highest surface Ni/Cu atomic ratio, indicating the presence of more highly dispersed Ni species deposited on TiO_2 support.

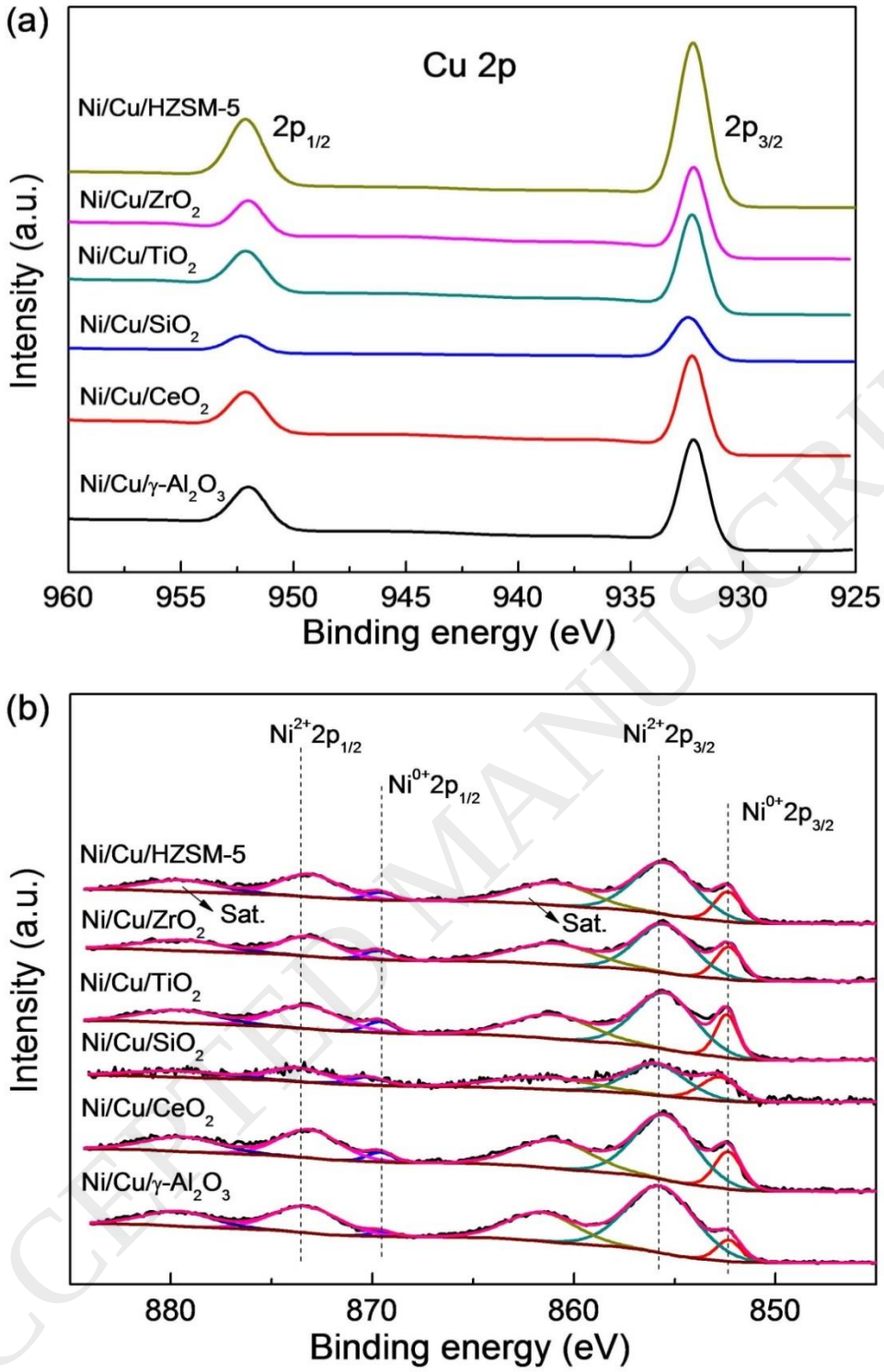

Figure 5. Cu 2p (a) and Ni 2p (b) XPS profiles of reduced supported bimetallic Ni/Cu catalysts.

3.2. Glycerol hydrogenolysis studies

3.2.1. Catalytic activity test

Table 2 presents the catalytic results for glycerol hydrogenolysis performed under different reaction conditions on supported bimetallic Ni/Cu catalysts. When the reactions were carried out under nitrogen pressure using 2-propanol as hydrogen source with a low glycerol concentration (*i.e.*, 5 wt% glycerol in 2-propanol), very high glycerol conversion (100%) was achieved on γ-Al_2O_3, TiO_2, and HZSM-5 supported bimetallic Ni/Cu catalysts (Entry 1, 4 and 6). In contrast, the Ni/Cu/CeO_2, Ni/Cu/SiO_2 and Ni/Cu/ZrO_2 catalysts exhibited a lower glycerol conversion (60-74%). Also, a high concentration of acetol (15–20% selectivity) was detected on these catalysts. Unlike them, the Ni/Cu/HZSM-5 catalyst showed a relatively low acetol selectivity (4.8%), but there existed large amounts of byproducts, which resulted in the decrease of 1,2-PDO selectivity. In addition, the catalytic activities of Ni/TiO_2 and 30Cu/TiO_2 catalysts were also investigated for comparative analysis. As can be seen, the glycerol conversion and 1,2-PDO selectivity for Ni/TiO_2 catalyst were 76.1% and 60.9%, respectively and greater than those obtained on 30Cu/TiO_2 catalyst (Entry 7 and 8). However, the selectivity to acetol for both Ni/TiO_2 and 30Cu/TiO_2 catalysts was very high, at 21% and 33% respectively, indicating that the hydrogenation of acetol to 1,2-PDO was restrained. Among the catalysts tested, Ni/Cu/γ-Al_2O_3 and Ni/Cu/TiO_2 catalysts obtained a higher catalytic activity, exhibiting 100% glycerol conversion with 73.7% and 82.2% 1,2-PDO selectivity respectively.

To further compare the catalytic activity of Ni/Cu/γ-Al_2O_3 and Ni/Cu/TiO_2 catalysts, the experiment was performed at a high glycerol concentration (*i.e.*, 10 wt% glycerol in 2-propanol). As clearly shown in Table 2, the activity of Ni/Cu/TiO_2 catalyst was higher than that of Ni/Cu/γ-Al_2O_3 catalyst from the perspective of glycerol conversion and selectivity to 1,2-PDO (Entry 9 and 10). Additionally, the reactions using acetol/2-propanol as reactant on the

Ni/Cu/γ-Al_2O_3 and Ni/Cu/TiO_2 catalysts were carried out to get a deeper understanding of the role of active sites on glycerol hydrogenolysis (Entry 11 and 12). In the case of Ni/Cu/γ-Al_2O_3 catalyst, the acetol conversion and 1,2-PDO selectivity were 85.2% and 59.4%, respectively. However, large amounts of byproducts were generated. In contrast, relatively high acetol conversion and 1,2-PDO selectivity, and less byproducts were achieved on Ni/Cu/TiO_2 catalyst, suggesting that the acetol hydrogenation activity of Ni/Cu/TiO_2 catalyst with low acidity was higher than that of Ni/Cu/γ-Al_2O_3 catalyst with high acid strength.

Table 2 Catalytic results of glycerol hydrogenolysis on supported bimetallic Ni/Cu catalysts

Entry	Catalyst	Conversion (%)	Selectivity (%)		
			1,2-PDO	Acetol	Others
1	Ni/Cu/γ-Al_2O_3	100	73.7	7.9	18.4
2	Ni/Cu/CeO_2	63.3	67.1	16.9	16.0
3	Ni/Cu/SiO_2	60.1	60.6	19.8	19.6
4	Ni/Cu/TiO_2	100	82.2	5.3	12.5
5	Ni/Cu/ZrO_2	74.3	69.4	15.2	15.4
6	Ni/Cu/HZSM-5	100	51.7	4.8	43.5
7	Ni/TiO_2	76.1	60.9	21.2	17.9
8	30Cu/TiO_2	52.5	57.2	32.8	10.0
9	Ni/Cu/γ-Al_2O_3[a]	77.9	65.6	13.7	20.7
10	Ni/Cu/TiO_2[a]	84.6	74.1	11.2	14.7
11	Ni/Cu/γ-Al_2O_3[b]	85.2	59.4	-	40.6
12	Ni/Cu/TiO_2[b]	93.7	68.6	-	31.4

13	Ni/Cu/γ-Al_2O_3[c]	25.7	28.9	17.2	53.9
14	Ni/Cu/TiO_2[c]	30.3	32.7	15.0	52.3
15	Ni/Cu/γ-Al_2O_3[d]	100	82.8	2.6	14.6
16	Ni/Cu/TiO_2[d]	100	86.5	1.4	12.1
17	Ni/Cu/γ-Al_2O_3[e]	84.2	87.3	3.5	9.2
18	Ni/Cu/TiO_2[e]	79.1	89.7	2.6	7.7
19	Ni/Cu/γ-Al_2O_3[f]	76.3	76.1	5.9	18.0
20	Ni/Cu/TiO_2[f]	68.9	79.4	5.1	15.5

Experimental parameters: glycerol concentration, 5 wt%; solvent, 2-propanol; feed rate of liquid mixture, 27.8 mL·h^{-1}; nitrogen flow rate, 50 mL·min^{-1}; catalyst mass, 6.0 g; preheater temperature, 230 ℃; reactor temperature, 230 ℃; reaction pressure, 3.5 MPa. Others include methanol, methane, ethylene glycol, *etc*. The uncertainty of conversion, 1%; the uncertainty of selectivity, 2%. [a] 10 wt% glycerol in 2-propanol, nitrogen flow rate, 50 mL·min^{-1}. [b] 10 wt% acetol in 2-propanol, nitrogen flow rate, 50 mL·min^{-1}. [c] 5 wt% glycerol in water, nitrogen flow rate, 50 mL·min^{-1}. [d] 10 wt% glycerol in 2-propanol, hydrogen flow rate, 50 mL·min^{-1}. [e] 5 wt% glycerol in water, hydrogen flow rate, 50 mL·min^{-1}. [f] 20 wt% glycerol in 2-propanol, hydrogen flow rate, 50 mL·min^{-1}.

Besides the study of glycerol hydrogenolysis aided by *in situ* hydrogen production via CTH (*i.e*, using 2-propanol as hydrogen source), the activity for glycerol hydrogenolysis with hydrogen generated from glycerol APR was also tested on Ni/Cu/γ-Al_2O_3 and Ni/Cu/TiO_2 catalysts (Table 2). Similar to the result of glycerol hydrogenolysis with hydrogen derived from CTH, the activity of Ni/Cu/TiO_2 in glycerol APR was superior to that of Ni/Cu/γ-Al_2O_3 catalyst (Entry 13 and 14). It

should be noted, however, that the activities of both Ni/Cu/γ-Al_2O_3 and Ni/Cu/TiO_2 catalysts in glycerol APR were far lower than those in glycerol hydrogenolysis with hydrogen produced from CTH (Entry 1 and 4). Finally, the Ni/Cu/γ-Al_2O_3 and Ni/Cu/TiO_2 catalysts were selected for glycerol hydrogenolysis with an external hydrogen supply to study the influence of inert/reactive atmosphere on the catalyst activity and reaction pathway. Clearly, in comparison to glycerol hydrogenolysis in the absence of hydrogen supply, the addition of external hydrogen led to a significant increase in glycerol conversion and 1,2-PDO selectivity (Entry 15–18). Furthermore, the selectivity to acetol was notably decreased, suggesting that the intermediate of glycerol hydrogenolysis, *i.e.*, acetol, can be hydrogenated to 1,2-PDO quickly in the case of external hydrogen addition. Additionally, it is worthy to mention that the Ni/Cu/γ-Al_2O_3 catalyst exhibited higher glycerol conversion than the Ni/Cu/TiO_2 catalyst (Entry 17–20). This was slightly different from the result of glycerol hydrogenolysis with hydrogen produced from CTH and APR.

According to literature [31,35–38], the acid-catalyzed hydrogenolysis of glycerol to 1,2-PDO in the presence of hydrogen follows the dehydration-hydrogenation reaction pathway. That is, the glycerol is firstly dehydrated to produce acetol on acid sites of support, and then the acetol is hydrogenated to obtain 1,2-PDO on metal active sites of catalyst. From the above analysis, it is clear that both acid and metal active sites have great impact on 1,2-PDO production from glycerol. Similarly, in the case of CTH and/or APR, the presence of more acid and metal active sites is very necessary for the conversion of glycerol to 1,2-PDO, because they involve not only glycerol hydrogenolysis but *in situ* hydrogen production as well. Furthermore, it has been documented that the catalyst with a higher acidity favors the conversion of glycerol, and the presence of highly dispersed metal species, such as Ni and Cu, is beneficial to the improvement of the hydrogen

producing efficiency [38–40]. However, it seems that the effects of the acid and metal active sites over the catalyst on glycerol hydrogenolysis to 1,2-PDO are slightly different based on our experimental results.

In this study, the Ni/Cu/γ-Al_2O_3 and Ni/Cu/HZSM-5 catalysts possessed a higher acid strength and exhibited 100% glycerol conversion for glycerol hydrogenolysis with hydrogen produced from CTH (Entry 1 and 6). In the case of the Ni/Cu/TiO_2 catalyst, the glycerol conversion was also 100% (Entry 4), although its acidity was greatly lower than those of Ni/Cu/γ-Al_2O_3 and Ni/Cu/HZSM-5 catalysts, as confirmed by NH_3-TPD. Furthermore, the Ni/Cu/SiO_2 catalyst with the lowest acidity also showed 60.1% glycerol conversion (Entry 3), suggesting that the acidity of catalyst did not noticeably affect the glycerol conversion. Beside the difference of acidity, there is a difference in the metal active sites on the catalytic surface, as verified by N_2O chemisorption and XPS analysis. As shown in Table 1, the Ni/Cu/TiO_2 catalyst had the highest Cu dispersion, whereas the Cu dispersion of Ni/Cu/SiO_2 was lowest. In addition, the Ni/Cu/TiO_2, Ni/Cu/HZSM-5, and Ni/Cu/γ-Al_2O_3 catalysts showed a higher surface Ni/Cu atomic ratio than other supported bimetallic Ni/Cu catalysts. It is well documented that the presence of large quantities of the Cu and Ni active sites on catalytic surface can provide high activities for the C–O bond hydrogenolysis and hydrogen production, respectively [21,28]. To illustrate this, the gaseous products were also analyzed by GC when the reactions were conducted under nitrogen pressure using 2-propanol as hydrogen source.

As displayed in Table S1, a higher concentration of hydrogen at reactor outlet was detected for reactions performed on Ni/Cu/TiO_2, Ni/Cu/HZSM-5 and Ni/Cu/γ-Al_2O_3 catalysts. This was in agreement with the result of surface Ni/Cu atomic ratio, indicating that the higher the surface

Ni/Cu atomic ratio, the higher the hydrogen production activity. Conversely, a high concentration of acetol was detected in the presence of the Ni/Cu/CeO_2, Ni/Cu/SiO_2 and Ni/Cu/ZrO_2 catalysts (Entry 2, 3, and 5), most probably due to the lack of available hydrogen for the hydrogenation of acetol to 1,2-PDO. To illustrate further the effect of metal active sites over the catalyst on glycerol hydrogenolysis, the activities of Ni/Cu/TiO_2 catalysts with different Ni contents were studied under nitrogen pressure using 2-propanol as hydrogen source. As indicated in Table 3, the glycerol conversion was significantly enhanced, whereas the selectivity to acetol decreased continuously with an increase in Ni content of Ni/Cu/TiO_2 catalyst, suggesting that the higher the Ni content, the higher the glycerol conversion. From the analysis above, we could infer that the effect of metal active sites over the catalyst on glycerol hydrogenolysis was higher than that of acid sites over the catalyst when the reaction was performed under nitrogen pressure using 2-propanol as hydrogen source with a low glycerol concentration.

Table 3 Effect of Ni content in Ni/Cu/TiO_2 catalyst on glycerol hydrogenolysis

Ni content	Conversion	Selectivity (%)		
(wt%)	(%)	1,2-PDO	Acetol	Others
5	25.3	70.4	15.8	13.8
10	39.1	74.3	14.1	11.6
20	65.0	78.5	12.5	9.0
30	84.6	74.1	11.2	14.7
40	90.1	66.3	6.7	27.0

Experimental parameters: glycerol concentration, 10 wt%; solvent, 2-propanol; feed rate of liquid mixture, 27.8 $mL \cdot h^{-1}$; nitrogen flow rate, 50 $mL \cdot min^{-1}$; catalyst mass, 6.0 g; preheater temperature,

230 ℃; reactor temperature, 230 ℃; reaction pressure, 3.5 MPa. Others include methanol, ethylene glycol, *etc*. The uncertainty of conversion, 1%; the uncertainty of selectivity, 2%.

It should be noted, however, that it is not the case for glycerol hydrogenolysis with addition of external hydrogen. As displayed in Table 2, the Ni/Cu/γ-Al_2O_3 catalyst with a higher acidity and a lower Cu dispersion showed higher glycerol conversion than the Ni/Cu/TiO_2 catalyst in the case of external hydrogen addition (Entry 17–20). One possible explanation for this was that the glycerol dehydration on acid sites of the catalyst might be the controlling step, because there existed large amounts of available hydrogen in the reaction system and leading to the acetol can be hydrogenated to 1,2-PDO easily. Unlike the addition of external hydrogen and *in situ* hydrogen production via CTH, the hydrogen needed for glycerol hydrogenolysis to 1,2-PDO under nitrogen pressure using water as a solvent was derived from APR of glycerol. This process consumed parts of the glycerol and resulted in a lower utilization rate of it. Furthermore, the hydrogen quantity generated from APR of glycerol on Ni/Cu/γ-Al_2O_3 and Ni/Cu/TiO_2 catalysts was found to be significantly lower than that derived from CTH (see Table S1). However, it should be pointed out that the activity in glycerol APR and the concentration of hydrogen in the gas phase for Ni/Cu/TiO_2 catalyst were higher than those for Ni/Cu/γ-Al_2O_3 catalyst. This is consistent with the results for reactions carried out under nitrogen pressure using 2-propanol as hydrogen source.

According to literature and our experimental results, the possible reaction pathway for glycerol hydrogenolysis with and without addition of external hydrogen on Ni/Cu/TiO_2 catalyst was illustrated in Scheme 1. With and without external hydrogen, all the reaction pathway includes the dehydration of glycerol to produce acetol and the hydrogenation of acetol to achieve 1,2-PDO. Nevertheless, the effects of the acid and metal active sites of the Ni/Cu/TiO_2 catalyst on the

glycerol dehydration and hydrogenation process are different. In the presence of external hydrogen, the glycerol dehydration is the controlling step, and the conversion of glycerol to 1,2-PDO is much influenced by the acid sites of the catalyst. In contrast, the metal active sites of the catalyst have a great impact on the activity for hydrogen production and also affect the glycerol hydrogenolysis with hydrogen *in situ* produced from CTH and glycerol APR. Given its high catalytic performance for glycerol hydrogenolysis with hydrogen generated from CTH, the Ni/Cu/TiO_2 catalyst was selected for further investigation.

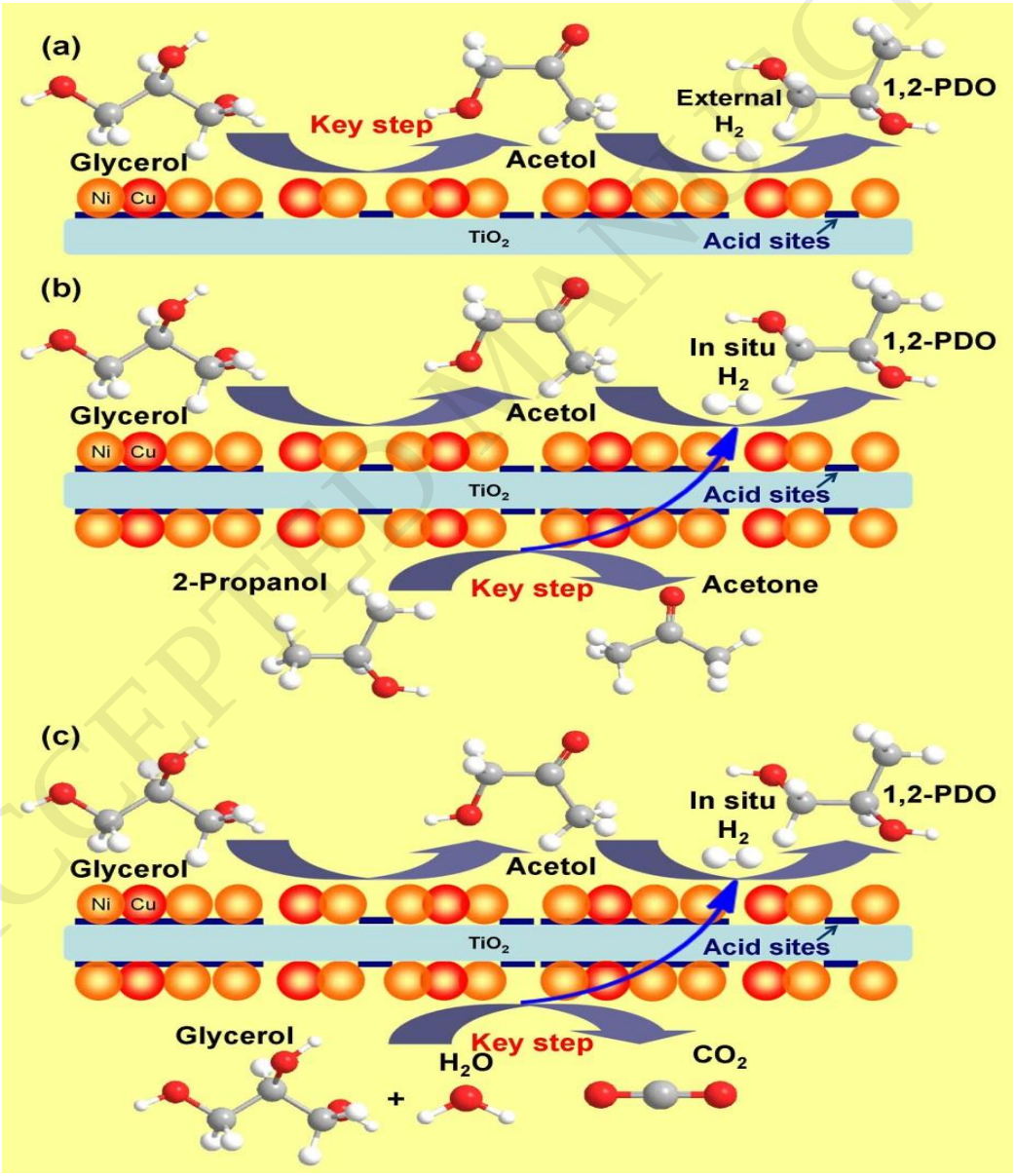

Scheme 1. Proposed reaction pathway for glycerol hydrogenolysis carried out on Ni/Cu/TiO_2

catalyst: addition of external hydrogen (a), *in situ* hydrogen production from CTH (b), and *in situ* hydrogen production from glycerol APR (c).

3.2.2. Effect of experimental parameters

Figure 6 shows the influence of different experimental parameters such as reaction temperature, glycerol concentration, and liquid flow rate on glycerol hydrogenolysis over Ni/Cu/TiO_2 catalyst under nitrogen pressure using 2-propanol as hydrogen source with a 10 wt% glycerol concentration. In Figure 6a, as expected, the glycerol conversion was notably raised from 36% to 100% when the reaction temperature was increased from 180 to 250 ℃, indicating that the enhancement of reaction temperature favored the increase in the conversion of glycerol. This might be related to the improved activity for hydrogen production with increasing reaction temperature [17]. However, the selectivity to 1,2-PDO was found to be enhanced at first and then decreased slightly with the increase in the reaction temperature. This might be ascribed to the high activity to break C-C bond of glycerol for Ni catalyst at high reaction temperature, which leads to the production of large amounts of undesired byproducts.

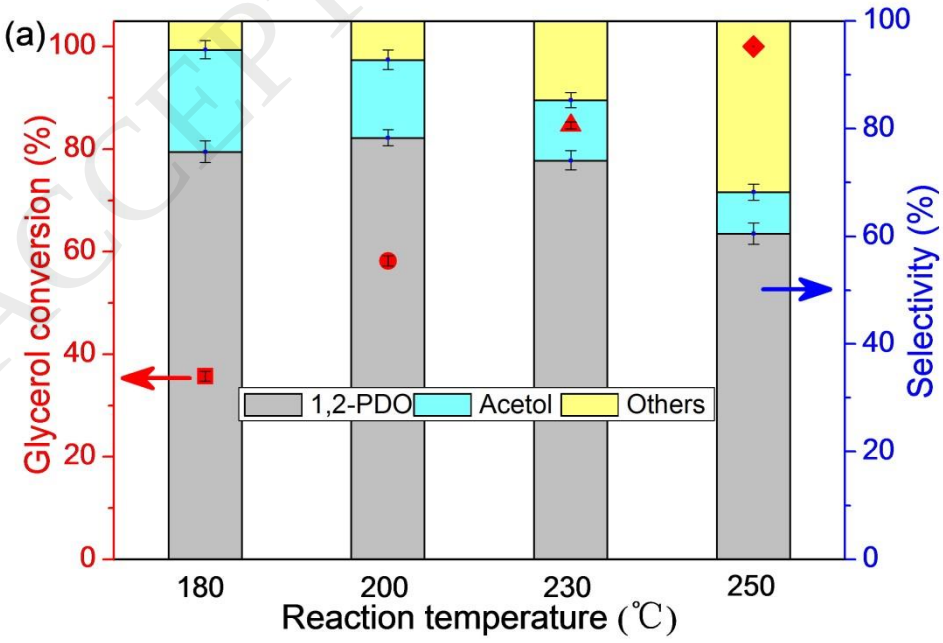

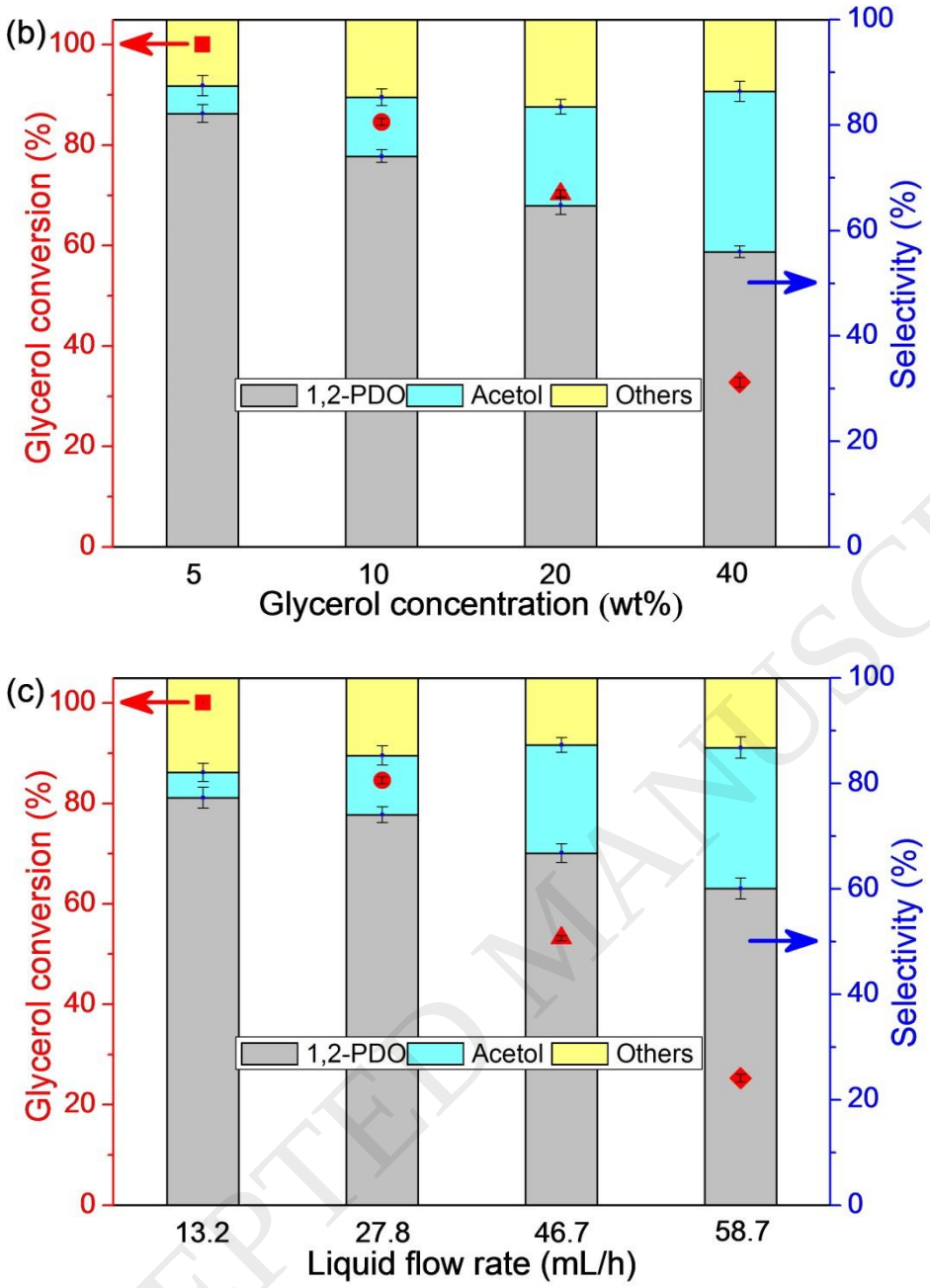

Figure 6. Influence of reaction temperature (a), glycerol concentration (b), and liquid flow rate (c) on glycerol hydrogenolysis over Ni/Cu/TiO_2 catalyst. Experimental parameters: glycerol concentration, 10 wt%; solvent, 2-propanol; feed rate of liquid mixture, 27.8 mL·h^{-1}; nitrogen flow rate, 50 mL·min^{-1}; catalyst mass, 6.0 g; preheater temperature, 230 ℃; reactor temperature, 230 ℃; reaction pressure, 3.5 MPa.

In Figure 6b, it was apparent that the increase in the glycerol concentration (5-40 wt%) resulted in a significant decrease in glycerol conversion from 100% to 33%. This was likely due to the

decrease of catalyst-to-glycerol ratio in the reaction system with the enhancement of glycerol concentration. In addition, the increasing glycerol concentration (*i.e.*, 2-propanol concentration decrease) can enhance the competitive adsorption of glycerol and 2-propanol on the active centers of the catalyst. It is expected that if glycerol adsorption is stronger, less 2-propanol would be adsorbed and lower H_2 would be generated with an increase in glycerol concentration. For this reason, due to lack of available hydrogen, the selectivity to 1,2-PDO gradually decreased from 82% to 56% when the glycerol concentration was enhanced from 5 wt% to 40 wt%. In contrast, the selectivity to acetol was improved at the expense of 1,2-PDO with the increase in glycerol concentration, indicating that the acetol generated from glycerol dehydration cannot be hydrogenated to 1,2-PDO, most probably due to the lack of available hydrogen. Similar to the effect of glycerol concentration on glycerol hydrogenolysis, the increase in liquid flow rate (13.2-58.7 $mL \cdot h^{-1}$) led to a notable decrease in glycerol conversion from 100% to 25% and selectivity to 1,2-PDO from 77% to 60%, respectively. The explanation for this could be attributed to the shorter residence time for glycerol over the catalyst surface at high liquid flow rate, which resulted in limited contact between the glycerol and catalyst.

3.2.3. Catalyst stability study

In this work, the stability of $Ni/Cu/TiO_2$ catalyst for glycerol hydrogenolysis with and without external hydrogen addition was studied at 230 ℃ and 3.5 MPa of operating pressure with a 5 wt% glycerol concentration. As clearly shown in Figure 7, the $Ni/Cu/TiO_2$ catalyst maintained the catalytic activity (in terms of glycerol conversion) over 60 h time on stream under N_2 pressure using 2-propanol as a solvent (*i.e*, glycerol hydrogenolysis with hydrogen produced from CTH). However, a significant deactivation was observed when the reaction time was increased to 68 h.

Similarly, the Ni/Cu/TiO_2 catalyst also showed obvious activity loss after 28 h of continuous operation under N_2 pressure using water as a solvent (*i.e*, glycerol hydrogenolysis with hydrogen derived from APR), despite relatively stable for 22 h time on stream at first. In contrast, regardless of the use of solvent, the stable operation time of glycerol hydrogenolysis with external hydrogen addition were prolonged, though the deactivation of Ni/Cu/TiO_2 catalyst still existed in the long run. This indicated that the stability of Ni/Cu/TiO_2 catalyst for glycerol hydrogenolysis with external hydrogen addition was higher than that with hydrogen generated from CTH and APR, consistent with their catalytic performance for glycerol hydrogenolysis.

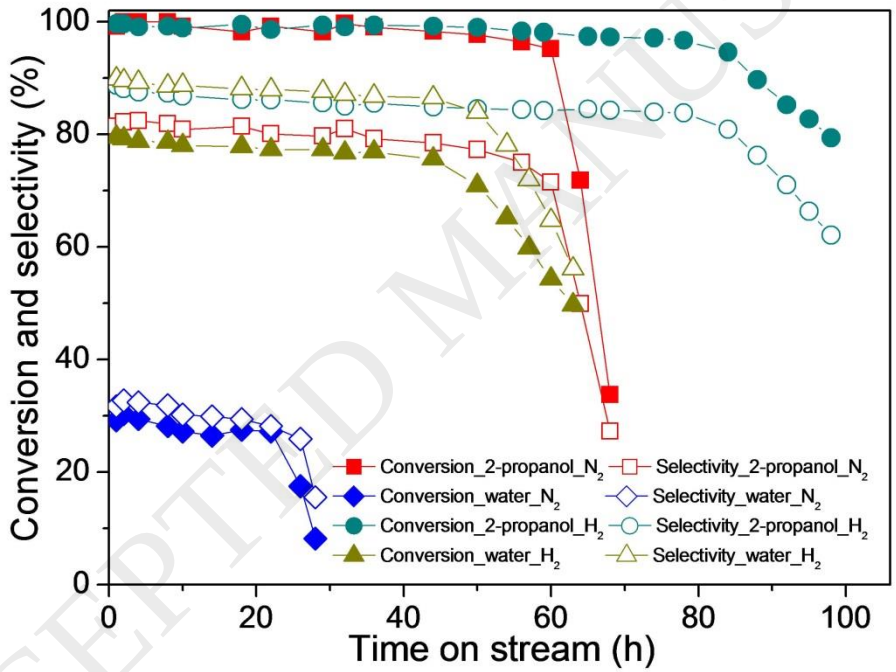

Figure 7. Stability test of Ni/Cu/TiO_2 catalyst. Experimental parameters: glycerol concentration, 5 wt%; solvent, 2-propanol or water; feed rate of liquid mixture, 27.8 mL·h^{-1}; N_2 or H_2 flow rate, 50 mL·min^{-1}; catalyst mass, 6.0 g; preheater temperature, 230 ℃; reactor temperature, 230 ℃; reaction pressure, 3.5 MPa.

At present, the deactivation of Cu-containing catalysts for glycerol hydrogenolysis with the addition of external hydrogen has been widely published in literature [41–44]. However, the

reason of catalyst deactivation for glycerol hydrogenolysis in the absence of external hydrogen supply has seldom been studied. To explore and clarify the deactivation phenomena in the present work, the used Ni/Cu/TiO_2 catalyst for glycerol hydrogenolysis with and without external hydrogen addition was analyzed using different techniques. Firstly, the spent catalyst was characterized by BET measurement. It was found that the BET surface area of the spent catalyst for glycerol hydrogenolysis was lower than that of the fresh catalyst (see Table S2), showing that parts of catalyst pores were blocked. Secondly, ICP-OES test for the used Ni/Cu/TiO_2 catalyst showed the presence of metal leaching, because the contents of Ni and Cu in the spent catalyst were lower than those in the fresh catalyst, and trace amounts of Ni and Cu were detected in the liquid product (see Table S2).

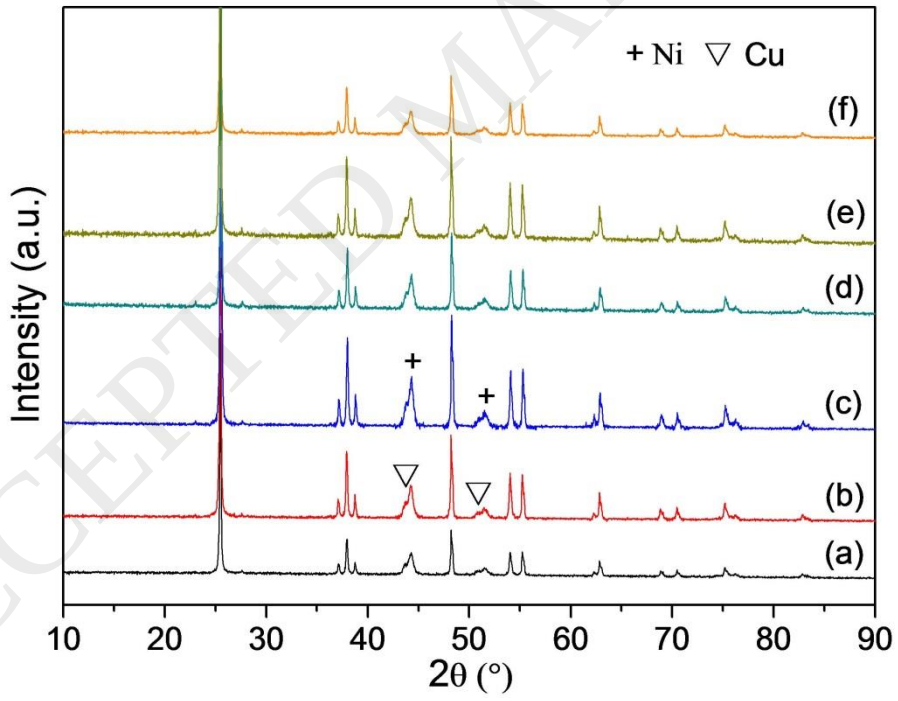

Figure 8. XRD patterns of reduced catalysts: fresh Ni/Cu/TiO_2 (a); spent Ni/Cu/TiO_2 after 68 h time on stream under N_2 pressure using 2-propanol as a solvent (b); spent Ni/Cu/TiO_2 after 28 h time on stream under N_2 pressure using water as solvent (c); spent Ni/Cu/TiO_2 after 98 h time on

stream under H_2 pressure using 2-propanol as a solvent (d); spent Ni/Cu/TiO_2 after 63 h time on stream under H_2 pressure using water as a solvent (e); spent Ni/Cu/TiO_2 after 50 h time on stream under N_2 pressure using 2-propanol as a solvent (f).

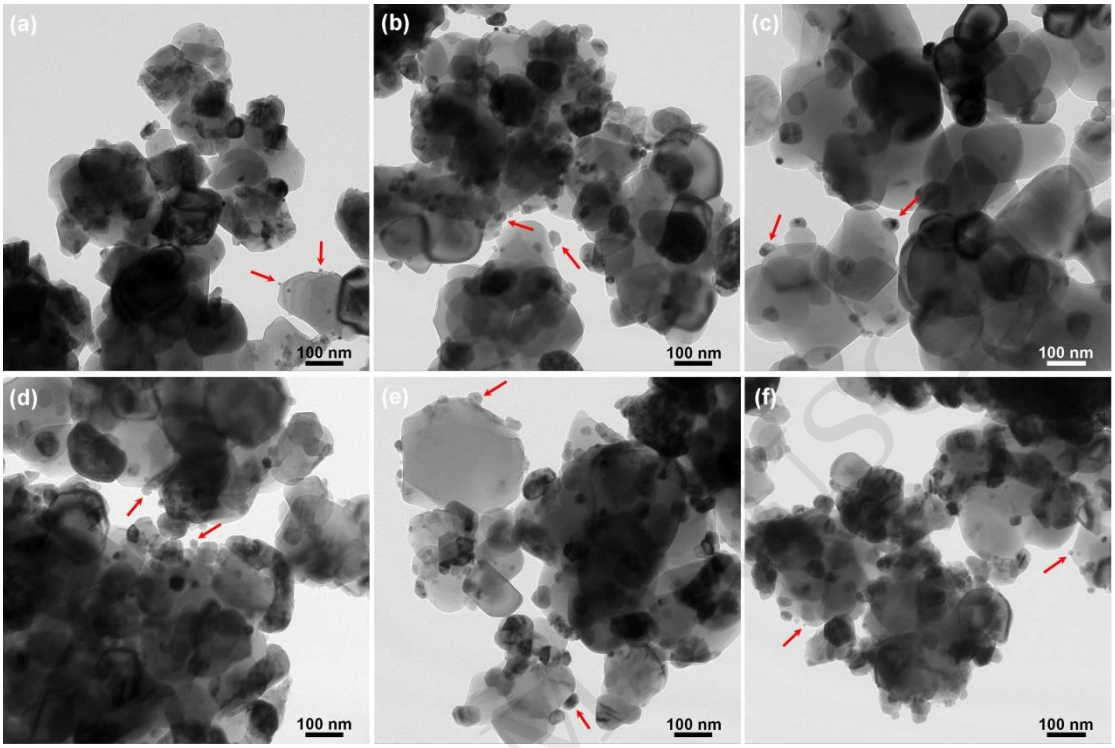

Figure 9. TEM images of catalysts: fresh Ni/Cu/TiO_2 (a); spent Ni/Cu/TiO_2 after 68 h time on stream under N_2 pressure using 2-propanol as a solvent (b); spent Ni/Cu/TiO_2 after 28 h time on stream under N_2 pressure using water as solvent (c); spent Ni/Cu/TiO_2 after 98 h time on stream under H_2 pressure using 2-propanol as a solvent (d); spent Ni/Cu/TiO_2 after 63 h time on stream under H_2 pressure using water as a solvent (e); spent Ni/Cu/TiO_2 after 50 h time on stream under N_2 pressure using 2-propanol as a solvent (f).

In addition, the phase composition of the used Ni/Cu/TiO_2 catalyst was measured by XRD. As illustrated in Figures 8a-e, the intensities of the diffraction peaks for both Ni and Cu phases on the spent catalyst were greatly higher than those of fresh catalyst, suggesting the presence of metal particles sintering. Meanwhile, regardless of the use of reaction atmosphere (*i.e.*, N_2 or H_2), the

degree of metal particles sintering for glycerol hydrogenolysis in the case of water as a solvent was higher than that using 2-propanol as a solvent according to the corresponding diffraction peak intensity. To illustrate this point, the used and fresh Ni/Cu/TiO_2 catalysts were submitted to TEM analysis. As displayed in Figures 9a-e, evident agglomerates were present on the used catalysts for glycerol hydrogenolysis, regardless of the use of solvent. Particularly, bigger metal particles were seen on the spent catalyst for glycerol hydrogenolysis using water as a solvent, despite less number of metal particles deposited on the support surface. The explanation for this could be due to the strong polarity of water and the presence of high metal leaching, in line with the ICP-OES analysis.

Besides the aforementioned characterization techniques, thermogravimetric analysis (TGA) for weight loss measurement was also performed, and the result is represented in Figure 10. According to literature [43–46], the initial weight loss below 200 ℃ was considered to be the removal of water in the catalyst, whereas the weight loss between 200 and 400 ℃ described the loss of absorbed species like glycerol and acetol oligomers deposited on the catalyst surface. Additionally, the weight loss above 400 ℃ can be ascribed to the presence of carbonaceous deposits. It is evident from Figure 10 that the weight losses between 200 and 400 ℃ on the used catalyst were about 12.5% and 8.5%, respectively for glycerol hydrogenolysis using water as a solvent after 63 h time on stream under H_2 pressure and after 28 h time on stream under N_2 pressure. In contrast, the corresponding weight loss reached about 15.6% and 19.1% respectively, when glycerol hydrogenolysis was performed using 2-propanol as a solvent after 98 h time on stream under H_2 pressure and after 68 h time on stream under N_2 pressure. Meanwhile, there were still some carbonaceous deposits on the catalyst surface (see Figure 10 and Table S2), suggesting

that the adsorbed species can be more easily attached to the spent catalyst when glycerol hydrogenolysis was carried out using 2-propanol as a solvent, resulting in the deactivation of catalyst.

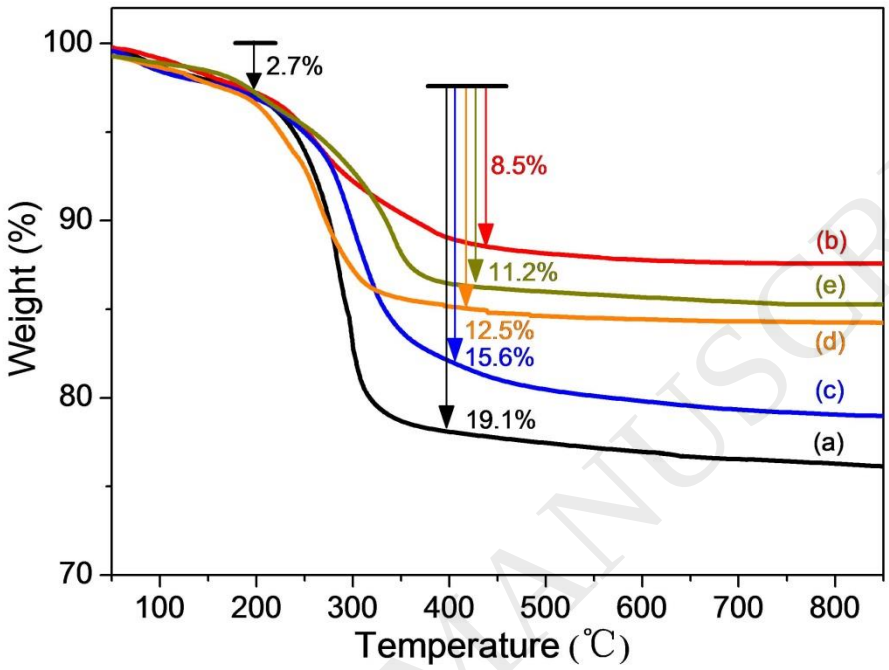

Figure 10. TGA curves of catalysts: spent Ni/Cu/TiO_2 after 68 h time on stream under N_2 pressure using 2-propanol as a solvent (a); spent Ni/Cu/TiO_2 after 28 h time on stream under N_2 pressure using water as solvent (b); spent Ni/Cu/TiO_2 after 98 h time on stream under H_2 pressure using 2-propanol as a solvent (c); spent Ni/Cu/TiO_2 after 63 h time on stream under H_2 pressure using water as a solvent (d); spent Ni/Cu/TiO_2 after 50 h time on stream under N_2 pressure using 2-propanol as a solvent (e).

The characterization results above indicate that the reason for catalyst deactivation in this study might be related to the metal leaching, metal particles sintering, and the presence of adsorbed species on the catalyst surface. The metal leaching and metal particles sintering were responsible for the catalyst deactivation when the glycerol hydrogenolysis was conducted using water as a

solvent, whereas the metal particles sintering and the presence of adsorbed species on the catalyst surface were considered to be the prime reasons for activity loss in the case of reaction performed using 2-propanol as a solvent.

It should be emphasized, however, that the deactivation (a sudden fall in activity) of $Ni/Cu/TiO_2$ catalyst in the CTH process (*i.e.*, glycerol hydrogenolysis under N_2 pressure using 2-propanol as a solvent) seems to be different from that in other glycerol hydrogenolysis processes. Likewise, in order to get a deeper understanding of the deactivation phenomenon, different characterization techniques were carried out to analyze the spent catalyst when the reaction was performed after 50 h time on stream under N_2 pressure using 2-propanol as a solvent, in which case the activity of $Ni/Cu/TiO_2$ catalyst was relatively stable. As shown in Figures 8f and 9f, the metal particles of spent $Ni/Cu/TiO_2$ catalyst can remain at approximately their original particle size. Meanwhile, the weight loss above 400 ℃ corresponding to the presence of carbonaceous deposits was very low (see Figure 10 and Table S2), despite also exhibiting 11.2% weight loss between 200 and 400 ℃. From the above analysis, the reason for sudden fall in activity in the CTH process might be associated with metal particles sintering and the presence of adsorbed species, especially carbonaceous deposits on the catalyst surface. In addition, it should be noted that the deactivation of $Ni/Cu/TiO_2$ catalyst for glycerol hydrogenolysis with external hydrogen addition was gradual (see Figure 7), regardless of the use of solvent. The explanation for this could be because the deactivation rate of catalyst to a certain extent was restrained by external hydrogen atmosphere. Nonetheless, the deactivation mechanism requires further study in the future, particularly, the deactivation (a rapid decrease in activity) of $Ni/Cu/TiO_2$ catalyst in the CTH process.

4. Conclusions

In this study, different supported bimetallic Ni/Cu catalysts were prepared for 1,2-PDO production from glycerol in a fixed-bed flow reactor, aided by *in situ* hydrogen production and also with addition of external hydrogen. The experiments of glycerol hydrogenolysis under nitrogen pressure using 2-propanol as hydrogen source indicated that the Ni/Cu/TiO_2 catalyst exhibited the highest 1,2-PDO yield, which was due to the high Cu dispersion and Ni/Cu atomic ratio on the catalyst surface. Furthermore, when the Ni content of the Ni/Cu/TiO_2 catalyst was enhanced, a significant increase in glycerol conversion was obtained. Unlike the reaction with addition of external hydrogen, where the effect of catalyst acid sites on glycerol hydrogenolysis was more noticeable, the metal active sites of the catalyst had a more significant positive impact on the activity for hydrogen production and also affected the glycerol hydrogenolysis with hydrogen produced from 2-propanol CTH and glycerol APR. The stability test over 28 h time on stream showed that the Ni/Cu/TiO_2 catalyst underwent serious deactivation for reaction performed under nitrogen pressure using water as a solvent. In contrast, the Ni/Cu/TiO_2 catalyst could stabilize to 60 h for glycerol hydrogenolysis with hydrogen generated from CTH. However, further increase in reaction time resulted in an obvious activity loss. The deactivation phenomena were also found in the case of glycerol hydrogenolysis with external hydrogen addition, regardless of the use of solvent. The characterization results suggested that the metal leaching and metal particles sintering were responsible for the catalyst deactivation when the reactions were conducted using water as a solvent. But the activity loss in the case of glycerol hydrogenolysis performed using 2-propanol as a solvent was mainly ascribed to the metal particles sintering and the presence of adsorbed species on the catalyst surface.

Acknowledgements

The authors gratefully acknowledge the National Natural Science Foundation of China (No. 21406034 and No. 21676054) and Shanghai Sailing Program (No. 18YF1425800) for the financial support.

References

[1] I. Kralova, J. Sjöblom, J. Disper. Sci. Technol. 31 (2010) 409–425.

[2] A. Demirbas, S. Karslioglu, Energ. Source Part A 29 (2007) 133–141.

[3] Y. Nakagawa, K. Tomishige, Catal. Sci. Technol. 1 (2011) 179–190.

[4] M. Pagliaro, R. Ciriminna, H. Kimura, M. Rossi, C.D. Pina, Angew. Chem. Int. Ed. 46 (2007) 4434–4440.

[5] C.-H. Zhou, J.N. Beltramini, Y.-X. Fan, G.Q. Lu, Chem. Soc. Rev. 37 (2008) 527–549.

[6] Y. Xiao, A. Varma, ACS Energ. Lett. 1 (2016) 963–968.

[7] J. ten Dam, U. Hanefeld, ChemSusChem 4 (2011) 1017–1034.

[8 T. Miyazawa, Y. Kusunoki, K. Kunimori, K. Tomishige, J. Catal. 240 (2006) 213–221.

[9] V.L. Yfanti, E.S. Vasiliadou, A.A. Lemonidou, Catal. Sci. Technol. 6 (2016) 5415–5426.

[10] J. Hu, Y. Fan, Y. Pei, M. Qiao, K. Fan, X. Zhang, B. Zong, ACS Catal. 3 (2013) 2280–2287.

[11] I. Gandarias, P.L. Arias, J. Requies, M. El Doukkali, M.B. Güemez, J. Catal. 282 (2011) 237–247.

[12] M.G. Musolino, L.A. Scarpino, F. Mauriello, R. Pietropaolo, Green Chem. 11 (2009) 1511–1513.

[13] S. Xia, L. Zheng, L. Wang, P. Chen, Z. Hou, RSC Adv. 3 (2013) 16569–16576.

[14] I. Gandarias, P.L. Arias, S.G. Fernández, J. Requies, M. El Doukkali, M.B. Güemez, Catal.

Today 195 (2012) 22–31.

[15] I. Gandarias, J. Requies, P.L. Arias, U. Armbruster, A. Martin, J. Catal. 290 (2012) 79–89.

[16] E. D'Hondt, S. Van de Vyver, B.F. Sels, P.A. Jacobs, Chem. Commun. 45 (2008) 6011–6012.

[17] F. Mauriello, A. Vinci, C. Espro, B. Gumina, M.G. Musolino, R. Pietropaolo, Catal. Sci. Technol. 5 (2015) 4466–4473.

[18] C. Pendem, P. Gupta, N. Chaudhary, S. Singh, J. Kumar, T. Sasaki, A. Datta, R. Bal, Green Chem. 14 (2012) 3107–3113.

[19] A. Seretis, P. Tsiakaras, Fuel Process. Technol. 142 (2016) 135–146.

[20] Y.S. Yun, D.S. Park, J. Yi, Catal. Sci. Technol. 4 (2014) 3191–3202.

[21] I.C. Freitas, R.L. Manfro, M.M. V.M. Souza, Appl. Catal. B Environ. 220 (2018) 31–41.

[22] F. Cai, G. Xiao, Catal. Sci. Technol. 6 (2016) 5656–5667.

[23] F. Cai, W. Zhu, G. Xiao, Catal. Sci. Technol. 6 (2016) 4889–4900.

[24] F. Cai, X. Song, Y. Wu, J. Zhang, G. Xiao, ACS Sustainable Chem. Eng. 6 (2018) 110–118.

[25 M. Balaraju, V. Rekha, B.L.A.P. Devi, R.B.N. Prasad, P.S.S. Prasad, N. Lingaiah, Appl. Catal. A Gen. 384 (2010) 107–114.

[26] N. Hamzah, N.M. Nordin, A.H.A. Nadzri, Y.A. Nik, M.B. Kassim, M.A. Yarmo, Appl. Catal. A Gen. 419–420 (2012) 133–141.

[27] R.V. Sharma, P. Kumar, A.K. Dalai, Appl. Catal. A Gen. 477 (2014) 147–156.

[28] S. Zhu, X. Gao, Y. Zhu, Y. Zhu, H. Zheng, Y. Li, J. Catal. 303 (2013) 70–79.

[29] M. Checa, A. Marinas, J.M. Marinas, F.J. Urbano, Appl. Catal. A Gen. 507 (2015) 34–43.

[30] H. Mitta, P.K. Seelam, S. Ojala, R.L. Keiski, P. Balla, Appl. Catal. A Gen. 550 (2018) 308–319.

[31] Y. Feng, H. Yin, A. Wang, L. Shen, L. Yu, T. Jiang, Chem. Eng. J. 168 (2011) 403–412.

[32] S. Kirumakki, B. Shpeizer, G. Sagar, K. Chary, A. Clearfield, J. Catal. 242 (2006) 319–331.

[33] H. Tan, M.N. Hedhill, Y. Wang, J. Zhang, K. Li, S. Sioud, Z.A. Al-Talla, M.H. Amad, T. Zhan, O.E. Tall, Y. Han, Catal. Sci. Technol. 3 (2013) 3360–3370.

[34] T. Jiang, Q. Huai, T. Geng, W. Ying, T. Xiao, F. Cao, Biomass Bioenerg. 78 (2015) 71–79.

[35] I. Gandarias, P.L. Arias, J. Requies, M.B. Güemez, J.L.G. Fierro, Appl. Catal. B Environ. 97 (2010) 248–256.

[36] M. Balaraju, V. Rekha, P.S.S. Prasad, B.L.A.P. Devi, R.B.N. Prasad, N. Lingaiah, Appl. Catal. A Gen. 354 (2009) 82–87.

[37] V. Montes, M. Boutonnet, S. Järås, A. Marinas, J.M. Marinas, F.J. Urbano, Catal. Today 257 (2015) 246–258.

[38] G.S. Foo, D. Wei, D.S. Sholl, C. Sievers, ACS Catal. 4 (2014) 3180–3192.

[39] E.S. Vasiliadou, V.L. Yfanti, A.A. Lemonidou, Appl. Catal. B Environ. 163 (2015) 258–266.

[40] E.S. Vasiliadou, E. Heracleous, I.A. Vasalos, A.A. Lemonidou, Appl. Catal. B Environ. 92 (2009) 90–99.

[41] C. Wang, H. Jiang, C. Chen, R. Chen, W. Xing, Chem. Eng. J. 264 (2015) 344–350.

[42] A. Bienholz, F. Schwab, P. Claus, Green Chem. 12 (2010) 290–295.

[43] E.S. Vasiliadou, A.A. Lemonidou, Appl. Catal. A Gen. 396 (2011) 177–185.

[44] E.S. Vasiliadou, T.M. Eggenhuisen, P. Munnik, P.E. de Jongh, K.P. de Jong, A.A. Lemonidou, Appl. Catal. B Environ. 145 (2014) 108–119.

[45] W. Suprun, M. Lutecki, T. Haber, H. Papp, J. Mol.Catal. A Chem. 309 (2009) 71–78.

[46] J. Zhou, J. Zhang, X. Guo, J. Mao, S. Zhang, Green Chem. 14 (2012) 156–163.